



## First Observations of Multi-harmonic Magnetosonic Waves with the Frequencies of Harmonics Higher than the Lower Hybrid Frequency

S. Y. Huang<sup>(1)</sup>, D. Deng<sup>(1)</sup>, Z. G. Yuan<sup>(1)</sup>, K. Jiang<sup>(1)</sup>, J. X. Li<sup>(2)</sup>,  
X. H. Deng<sup>(3)</sup>, X. D. Yu<sup>(1)</sup>, L. H. He<sup>(1)</sup>, Y. Y. Wei<sup>(1)</sup>, and S. B. Xu<sup>(1)</sup>

(1) School of Electronic Information, Wuhan University, Wuhan, China

(2) Department of Atmospheric and Oceanic Sciences, University of California, Los Angeles, USA

(3) Institute of Space Science and Technology, Nanchang University, Nanchang, China

### Abstract

Magnetosonic waves, with the frequency between proton cyclotron frequency and lower hybrid frequency, mainly occur near the Earth's magnetic equatorial plane, and play an important role in the magnetospheric dynamics. In this paper, we report unusual magnetosonic waves observed by Magnetospheric Multiscale (MMS) mission in the magnetotail. These magnetosonic waves have multi-band enhanced electromagnetic power spectral densities with the frequency from below to above the lower hybrid frequency, and are quasi-perpendicular propagating and linear polarized. The frequency of fundamental band is much higher than the proton cyclotron frequency  $f_{ci}$  (i.e.,  $35.2f_{ci}$ ). We identified these emissions as high frequency multi-harmonic magnetosonic waves. This is the first time for the observations of such high frequency multi-harmonic magnetosonic waves with the frequencies of harmonics higher than the lower hybrid frequency in the Earth's magnetosphere to the best of our knowledge. In view of the absence of ring distributions for the protons and the easy coupling between compressed mode and its electromagnetic term, we propose that the harmonic structures of the observed magnetosonic waves are generated by the non-linear wave-wave coupling among electromagnetic terms of the fundamental and higher harmonic waves via the wavelet bicoherence analysis method.

### 1 Introduction

Magnetosonic waves are frequently occurring in the Earth's magnetosphere (Russell et al., 1969). Since the discovery of magnetosonic waves was decades ago, a great deal of research has been carried out, including theoretical work, simulations, and observations on the magnetosonic waves (Boardsen et al., 1992; Horne et al., 2000; Yuan et al., 2017). Generally, magnetosonic waves are linear polarized and propagating quasi-perpendicularly to the ambient magnetic field. The frequency range of magnetosonic waves is usually between the proton cyclotron frequency and the lower hybrid frequency (e.g., Perraut et al., 1982). Magnetosonic waves sometimes have harmonic structures, but are often unstructured continuous spectrum (e.g., Balikhin et al., 2015). Although that magnetosonic waves are confined in small latitude regions, magnetosonic waves can fulfill most of the equatorial plane due to their propagation in the radial

and azimuthal directions, thus these waves play an important role in the evolution of the magnetospheric particles (e.g., Chen et al., 2015; Horne et al., 2007; Li et al., 2016).

Based on the observation from Magnetospheric Multiscale (MMS) mission, one new type of multi-harmonic magnetosonic waves, with the frequencies of harmonics higher than the lower hybrid frequency, are detected in the magnetotail plasma sheet. Through wavelet bicoherence analysis, the harmonics of magnetosonic waves are possibly generated by non-linear wave-wave interaction coupling between the electromagnetic terms of the fundamental mode and harmonics.

### 2 MMS Observations

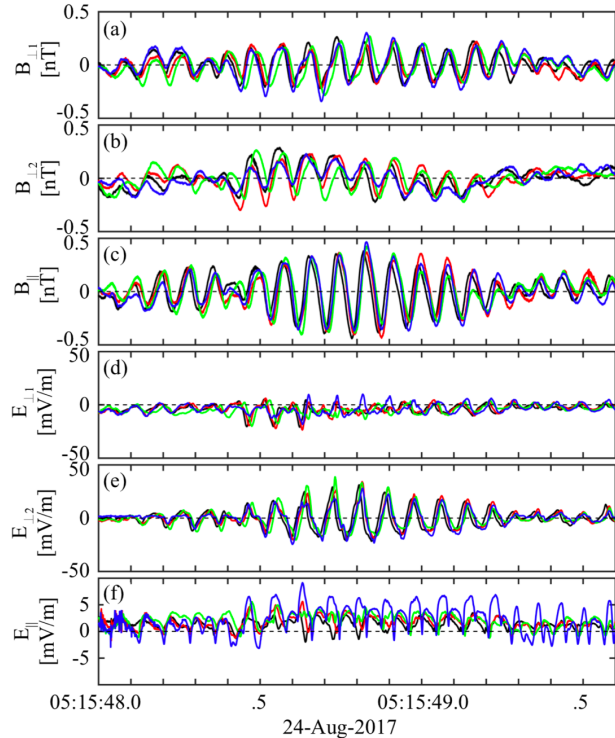
The data from MMS mission in burst mode from MMS are used in this study.

Figure 1 displays the perturbed magnetic and electric fields in the field-aligned coordinate (FAC) system. It is found that the parallel perturbed magnetic fields (the amplitude is up to 0.5 nT, Figure 1c) are larger than the perpendicular perturbed magnetic field (Figure 1a-b), while the perpendicular electric fields (the amplitude is up to 40 mV/m, Figure 1d-e) are much larger than the parallel electric field (Figure 1f). The unipolar parallel electric field occurs during this time interval. The unipolar changes in  $E_{\parallel}$  has also been reported in parallel electric field of the whistlers (e.g. Kellogg et al., 2010; An et al., 2019).

To show the wave properties in more detail, we calculated the power spectral density (PSD) of electric and magnetic fields via Fast Fourier Transformation (FFT), which is shown in Figure 2a. Blue line represents PSD of magnetic field, and red line represents PSD of electric field. There are at least two peaks in the PSD of magnetic field with the central frequencies at  $f_1 = 11.6$  Hz ( $f_1 = 35.2f_{ci}$ , where  $f_{ci} = 0.33$  Hz is proton cyclotron frequency), and  $f_2 = 23.2$  Hz ( $f_2 = 70.3f_{ci}$ ), and four peaks in the PSD of electric field with the central frequencies at  $f_1 = 11.6$  Hz,  $f_2 = 23.2$  Hz,  $f_3 = 34.5$  Hz, and  $f_4 = 46.5$  Hz. It is easy to find that  $f_2, f_3$ , and  $f_4$  fall on the harmonics of  $f_1$ , in other words,  $f_2 = 2f_1$ ,  $f_3 = 3f_1$ , and  $f_4 = 4f_1$ . Especially, the fundamental band

observed here has enhanced spectrum at the frequency close to the lower hybrid frequency ( $f_{lh}=14.2$  Hz), while the frequencies of higher bands are higher than the lower hybrid frequency. The polarization analysis of the electric field has been performed, and the result suggests that these observed waves are linear polarized (Figure 2b). All features are similar to the typical features of magnetosonic waves except that the frequencies of observed harmonics are higher than the lower hybrid frequency.

Minimum variance analysis (MVA, Sonnerup and Scheiblev, 1998) method is used to calculate the wave vector of magnetic field fluctuations. As a result, the eigenvectors corresponding to the minimum eigenvalue  $\lambda_3$ , namely the unit vector of the wave vector, are found as (0.52, 0.75, 0.41) in GSM coordinates. Thus, the angle between the wave vector and the ambient magnetic field is  $89.3^\circ$ , which implies that the waves are perpendicular propagating with respect to the ambient magnetic field. Moreover, we perform the timing analysis on the magnetic field and electric field data of four MMS spacecraft. The angles between the propagation direction of the waves and the ambient magnetic field are about  $90^\circ$ , and the wave phase velocity is about  $1236 \pm 103$  km/s. For the second band, the angle between the direction of wave propagation and the ambient magnetic field is  $94.9^\circ$ , and the phase velocity is about  $1223 \pm 271$  km/s. Thus, the derived features of the second band are similar to the ones of the fundamental band, which suggests that the fundamental and second band belong to multi-harmonic modes. Due to the low spectral densities of higher bands, one cannot perform any more analysis on the fields.



**Figure 1.** The perpendicular and parallel components of

the electromagnetic field during 05:15:48-05:15:49.6 UT; (a-b) the perturbed perpendicular magnetic field components; (c) the perturbed parallel magnetic field component; (d-e) the perturbed perpendicular electric field components and (f) the perturbed parallel electric field.

Combined with the multi-harmonic structures at the power spectral density with the frequency around lower hybrid frequency, oblique propagation angles ( $\sim 90^\circ$ ) and linear polarization, as well as the fact that the parallel perturbed magnetic field is larger than the perpendicular one, and the perpendicular electric field is much larger than the parallel one, we conclude that the observed emissions in the magnetotail plasma sheet is magnetosonic mode with high-frequency multi-harmonics (higher than the lower hybrid frequency). It is the first time that such high-frequency multi-harmonics magnetosonic wave, with the frequencies of harmonics higher than the lower hybrid frequency, is observed in the magnetosphere.

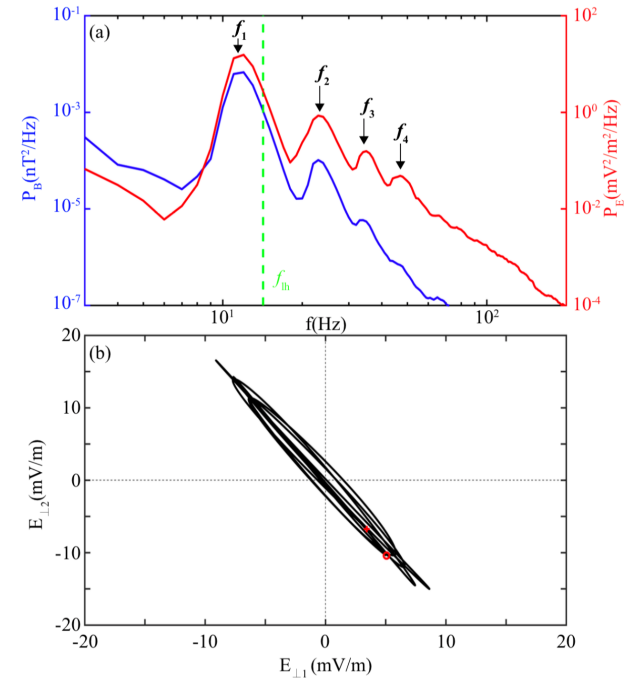


**Figure 2.** The properties of electromagnetic fluctuations. (a) Power spectral densities (PSDs) for electric ( $E_z$ ) and magnetic fields ( $B_x$ ) (green dotted line marks the lower hybrid frequency); (b) polarization analysis of electric field in the perpendicular plane (the red cross presents the start point, and the red cycle presents the end point).

Since the frequencies of the harmonics are much higher than  $f_{lh}$ , nonlinear generation mechanisms are recommended to excite these emissions. The perpendicular electric field (parallel perturbed magnetic field) are much larger than the parallel (perpendicular) ones, which indicates that the observed waves belong to compression mode. In view of that the compression wave mode itself is easily coupled with its own electromagnetic terms, non-linear wave-wave coupling may explain the

generation of these magnetosonic waves (Gao et al., 2017). Wavelet bicoherence analysis is an effective method for quantitative measurement of phase coupling between wave-wave modes, and has been widely used in many previous studies (Milligen et al., 1995; Gao et al., 2016, 2017). We established a new coordinate system: Z axis is along the direction of the background magnetic field  $\mathbf{B}_0$ , Y axis equals to  $(\mathbf{k} \times \mathbf{B}_0)$ , where  $\mathbf{k}$  denotes the wave vector, and X axis completes the right-hand coordinate system. The waveform data of parallel magnetic field ( $B_z$ ) and electric field along wave vector direction ( $E_x$ ) are selected to calculate the wavelet bicoherent index (Gao et al., 2017). Accordingly, the bicoherent index is defined as (Milligen et al., 1995):

$$\text{bicoherent index} = \frac{|\langle E_x(f_a)B_z(f_b)B_z^*(f_c) \rangle|^2}{\langle |E_x(f_a)B_z(f_b)|^2 \rangle \langle |B_z^*(f_c)|^2 \rangle}$$

where  $f_c = f_a + f_b$ ,  $B_z^*(f_c)$  is the conjugate pair of  $B_z(f_c)$ , and the bracket  $\langle \rangle$  denotes an average over the time interval of the observed waves. It introduces the bicoherent index to indicate the wave phase coupling: when the waves satisfy the resonance condition, the bicoherent index is close to 1, indicating strong wave-wave coupling; when the bicoherent index is close to 0, indicating no wave-wave coupling (Milligen et al., 1995).

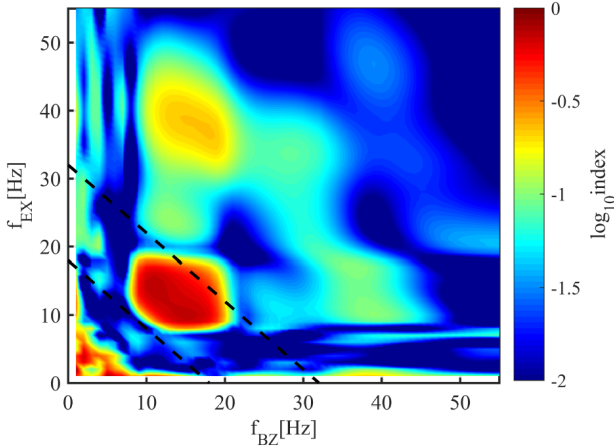


**Figure 3.** The distribution of bicoherent index between  $E_x$  and  $B_z$  components. Two dashed lines mark  $f_{Ex} + f_{Bz} = 18$  Hz and  $f_{Ex} + f_{Bz} = 32$  Hz, respectively.

Figure 3 shows the distribution of the wavelet bicoherent index in the  $f_{Bz}$ - $f_{Ex}$  plane. It is clearly shown that the maximum bicoherent index of wavelet analysis is in the overlap region of  $f_{Bz} = 8$ -18 Hz,  $f_{Ex} = 8$ -18 Hz, and  $f_{Bz} + f_{Ex} = 18$ -32 Hz (covers the frequencies of the second harmonic  $f_2 = 23.2$  Hz). This suggests strong coupling among the electromagnetic fields of the fundamental waves which leads to the generation of the second harmonic with the frequency between 18 and 32 Hz. It is worth noting that the power spectral density of second harmonic is two orders of magnitude smaller than the one of fundamental harmonic, and the power spectral density of third harmonic is about one order smaller than the one of the second harmonic, which leads to the power spectral density of the third harmonic so small that the coupling between higher harmonics is not easily observed in Figure 3. Therefore, we suggest that the harmonic structures of the high frequency magnetosonic wave are

excited by the nonlinear wave-wave interactions between the electric and magnetic terms of the fundamental or the harmonics.

### 3 Conclusions

Based on the observations of the MMS mission during 05:15:48 - 05:15:49.6 UT on August 24, 2017, one new type of high-frequency magnetosonic waves with multi-harmonics in the magnetotail plasma sheet has been investigated in detail. By means of calculating the power spectral density, polarization analysis, MVA and timing analysis, it is found that these waves have the typical properties of magnetosonic wave, such as perpendicular propagation, linear polarization and large parallel perturbed magnetic field and large perpendicular perturbed electric field, except for that the frequencies of harmonics are larger than the lower hybrid frequency. The frequency of fundamental band is much higher than the local proton cyclotron frequency (i.e.,  $f_1 = 35.2f_{ci}$ ). Thus, we identify these waves as high-frequency magnetosonic waves with multi-harmonic structures, i.e. high frequency multi-harmonic magnetosonic waves. We should point out that this event is not unique. We identified at least five events of such magnetosonic waves. However, due to the limited burst mode data during the tail season of MMS (i.e., from May to August in 2017), a statistical study could not be carried out. We proposed the excitation mechanism of this new magnetosonic wave is non-linear wave-wave interaction coupling via the wavelet bicoherence analysis method. More observations, theory and simulations are required to further investigate the high frequency multi-harmonic magnetosonic waves and possible wave-particle interactions in the magnetosphere in future.

### 4 Acknowledgements

We thank the entire MMS team and instrument leads for data access and support. This work was supported by the National Natural Science Foundation of China (41674161, 41874191), the project supported by the support by Young Elite Scientists Sponsorship Program by CAST (2017QNRC001), and the national youth talent support program. SYH thanks Dr. X. L. Gao for the helpful discussions.

### 5 References

1. X., An, Li, J., Bortnik, J., Decyk, V., Kletzing, C., & Hospodarsky, G., A unified view of nonlinear wave structures associated with whistler-mode chorus. *Physical Review Letters*, 2019, 122, 045101.
2. M. A., Balikhin, Y. Y. Shprits, S. N. Walker, et al. Observations of discrete harmonics emerging from equatorial noise, *Nat. Commun.* 2015, 6, 7703

3. L. Chen, Maldonado, A., Bortnik, J., Thorne, R. M., Li, J., Dai, L., & Zhan, X. Nonlinear bounce resonances between magnetosonic waves and equatorially mirroring electrons. *Journal of Geophysical Research: Space Physics*, 2016, 120, 6514–6527.
4. X. Gao, Q. Lu, J. Bortnik, W. Li, L. Chen, and S. Wang, Generation of multiband chorus by lower band cascade in the Earth's magnetosphere, *Geophys. Res. Lett.*, 2016, 43, 2343–2350, doi:10.1002/2016GL068313.
5. X. Gao, Ke, Y., Lu, Q., Chen, L., & Wang, S. Generation of multiband chorus in the Earth's magnetosphere: 1-D PIC simulation. *Geophysical Research Letters*, 2017, 44(2), 618–624. <https://doi.org/10.1002/2016GL072251>.
6. R. B., Horne, Thorne, R. M., Glauert, S. A., Meredith, N. P., Pokhotelov, D., & Santolik, O. Electron acceleration in the Van Allen radiation belts by fast magnetosonic waves. *Geophysical Research Letters*, 2007, 34, L17107.
7. S. Y., Huang, Z.G. Yuan, B. Ni, M. Zhou, H.S. Fu, S. Fu, X.H. Deng, Y. Pang, H.M. Li, D.D. Wang, H.M. Li, X.D. Yu, Observations of large-amplitude electromagnetic waves and associated wave-particle interactions at the dipolarization front in the Earth's magnetotail: A case study, *J Atmos Sol-Terr Phy*, 2015, 129, 119-127, doi:10.1016/j.jastp.2015.05.007
8. P. J., Kellogg, Cattell, C. A., Goetz, K., Monson, S. J., & Wilson III, L. B. Electron trapping and charge transport by large amplitude whistlers. *Geophysical Research Letters*, 2010, 37(20).
9. J., Li, Bortnik, J., Thorne, R. M., Li, W., Ma, Q., Baker, D. N., ... Blake, J. B. Ultrarelativistic electron butterfly distributions created by parallel acceleration due to magnetosonic waves. *Journal of Geophysical Research: Space Physics*, 2016, 121, 3212–3222. <https://doi.org/10.1002/2016JA022370>
10. B. P., Milligen, E. Sanchez, T. Estrada, C. Hidalgo, B. Branas, B. Carreras, and L. Garcia, Wavelet bicoherence: A new turbulence analysis tool, *Phys. Plasmas*, 1995, 2, 3017–3032.
11. S., Perraut, Roux, A., Robert, P., Gendrin, R., Sauvaud, J.- A., Bosqued, J.- M., Kremser, G., and Korth, A. A systematic study of ULF Waves Above FH+ from GEOS 1 and 2 Measurements and Their Relationships with proton ring distributions, *J. Geophys. Res.*, 1982, 87(A8), 6219–6236
12. C. T., Russell, Holzer, R. E., and Smith, E. J. OGO 3 observations of ELF noise in the magnetosphere: 1. Spatial extent and frequency of occurrence, *J. Geophys. Res.*, 1969, 74(3), 755–777, doi:10.1029/JA074i003p00755.
13. B. U. O., Sonnerup, & Scheible, M. Minimum and maximum variance analysis. In G. Paschmann & P. W. Daly (Eds.), *Analysis Methods for Multi-Spacecraft Data*, No. SR-001 in ISSI Scientific Reports (Chap. 1, pp. 185–220). (1998). Noordwijk, Netherlands: ESA Publications Division.
14. Z., Yuan, X. Yu, S. Huang, D. Wang, and H. O. Funsten, In situ observations of magnetosonic waves modulated by background plasma density, *Geophys. Res. Lett.*, 2017, 44, 7628–7633, doi:10.1002/2017GL074681.
15. Z., Yuan, X. Yu, S. Huang, Z. Qiao, F. Yao and H. O. Funsten, Cold ion heating by magnetosonic waves in a density cavity of the plasmasphere, *J. Geophys. Res. Space Physics*, 2018, 123, 1242-1250, <http://doi.org/10.1002/2017JA024919>.